

Supplementary Information for

Tailoring Solvation Chemistry towards Concurrent Hydrolysis-Free

I⁻/I⁺ Redox and Reversible Zn Anode in Zn–I₂ Batteries

Zhihao Zhao,^a Fanglin Wu,^b Huihua Li,^a Huang Zhang^{*a}

^a School of Electrical and Electronic Engineering, Harbin University of Science and Technology, Harbin 150080, China

* E-mail address: zhang.huang@hrbust.edu.cn

^b State Key Laboratory of Advanced Technology for Materials Synthesis and Processing, Wuhan University of Technology, Wuhan 430070, China

Experimental section

Chemicals

The zinc foils (Zn, 99.99%, Anhui Zhengying Technology Co., Ltd), copper foils (Cu, 99.99%, Canrd), zinc sulfate heptahydrate ($\text{ZnSO}_4 \cdot 7\text{H}_2\text{O}$, 99.995%, Aladdin), tetramethylammonium iodide (TMAI, 99%, Adamas), N,N-Dimethylacetamide (DMA, 99.8%, Adamas), Sodium Chloride (NaCl, 99.5%, Adamas), activated carbon (AC, YP-50F), iodine powder (I_2 , 99.995%, Adamas) and titanium mesh (Tianjin EVS Chemical Technology Co., Ltd) were used as purchased.

Electrolyte Preparation

Preparation of baseline electrolyte (BE): An appropriate amount of zinc sulfate heptahydrate ($\text{ZnSO}_4 \cdot 7\text{H}_2\text{O}$) reagent was accurately weighed, slowly added to specific deionized water, and stirred on a magnetic stirrer until completely dissolved to prepare a $2 \text{ mol L}^{-1} \text{ ZnSO}_4$ electrolyte, denoted as BE. Preparation of chloride-containing electrolyte (BE-NaCl): Corresponding masses of $\text{ZnSO}_4 \cdot 7\text{H}_2\text{O}$ and sodium chloride (NaCl) reagents were weighed in proportion, added together to specific deionized water, and magnetically stirred until both solutes were completely dissolved, obtaining a mixed electrolyte with component concentrations of $2 \text{ mol L}^{-1} \text{ ZnSO}_4$ - $0.5 \text{ mol L}^{-1} \text{ NaCl}$, denoted as BE-NaCl. Preparation of multicomponent hybrid electrolyte (HE): First, a mixed solvent was prepared by accurately measuring specific deionized water and N,N-dimethylacetamide (DMA) at a mass ratio of 3:1, mixed uniformly and stirred until the system was stable. Subsequently, $\text{ZnSO}_4 \cdot 7\text{H}_2\text{O}$, NaCl, and tetramethylammonium iodide (TMAI) reagents were sequentially added to this mixed solvent, magnetically stirred until all solutes were completely dissolved to ensure a homogeneous and transparent system. Moreover, the control electrolyte with a composition of $2 \text{ mol L}^{-1} \text{ ZnSO}_4$, $0.5 \text{ mol L}^{-1} \text{ NaCl}$, and $0.1 \text{ mol L}^{-1} \text{ TMAI}$ was prepared and denoted as BE-NaCl-TMAI. The electrolyte with a composition of $2 \text{ mol L}^{-1} \text{ ZnSO}_4$, $0.5 \text{ mol L}^{-1} \text{ NaCl}$, and 25% DMA was prepared and denoted as BE-NaCl-DMA.

Preparation of I_2 cathode material

An iodine-impregnated carbon composite cathode was prepared by thoroughly mixing 600 mg of activated carbon (AC) with 400 mg of iodine powder (I_2), followed by heat treatment at $90 \text{ }^\circ\text{C}$ for 6 h in a sealed glass vial. After cooling naturally to room temperature, the resulting $\text{I}_2@\text{AC}$ composite was mixed with Super P conductive carbon (Timcal) and polytetrafluoroethylene (PTFE, Canrd) binder at a mass ratio of 8:1:1. The mixed powder was ground thoroughly and fibrillated under shear to tightly bind the activated carbon with the conductive agent. The mixture was then compacted and repeatedly roll-pressed in a twin-roll press to the target thickness. The rolled sheet was pressed onto a titanium mesh to obtain the electrode. The final dry-processed cathode exhibited an areal mass loading of approximately $4\text{-}5 \text{ mg cm}^{-2}$, and the resulting electrode sheets were cut into discs ($\Phi 12 \text{ mm}$).

Electrochemical measurements

Electrochemical properties were evaluated at room temperature using 2032-type coin cells. Zn||Zn symmetric cells were fabricated using two identical Zn foils ($\phi 16\text{mm}$) sandwiched with a piece of Whatman GF/D glass fiber disc ($\phi 18\text{mm}$) with

various electrolytes. Zn||Cu asymmetric cells were also fabricated following the same procedure as symmetric cells, with the sole difference being the replacement of counter electrodes with Cu foils (\varnothing 12 mm). Zn-I₂ cells were assembled using an I₂@AC cathode, a Whatman GF/D glass fiber filter, and a Zn-foil anode (100 μ m thick), with 100 μ L of electrolyte. Galvanostatic charge/discharge tests were conducted on a Neware battery test system, within an electrochemical window of 0.6–1.9 V. Cyclic voltammetry (CV) and chronoamperometry (CA) measurements were performed on a CHI 660F electrochemical workstation, with a voltage range of 0.6–1.9 V for CV and a bias voltage of –150 mV for CA. Electrochemical impedance spectroscopy (EIS) was carried out on the CHI 660F electrochemical workstation, in a frequency range of 0.01 Hz to 100 kHz.

Material characterization

X-ray diffraction (XRD, Rigaku SmartLab SE) was used to characterize the side products on the Zn foil. Scanning electron microscopy (SEM, TESCAN MIRALMS) was employed to characterize the surface morphology change of the zinc anode. Ultraviolet-visible (UV-Vis, Hitachi UH4150) spectroscopy was used to monitor the changes in I-Cl species. In-situ Raman spectra were acquired using a confocal Raman microscope (alpha 300 R, Germany) with an argon-ion laser operating at a wavelength of 532 nm.

Computational methods

All calculations were performed using the Gaussian 16 software package. For all computations, Becke's three-parameter hybrid exchange functional combined with the Lee-Yang-Parr correlation functional (B3LYP) was employed, along with Grimme's D3 dispersion correction incorporating Becke-Johnson damping (DFT-D3BJ). Geometry optimization and frequency calculations were performed using the 6-31G+(d, p) basis set with the PCM solvation model to account for the DMA:H₂O = 25:94 solvent environment. Single-point energy calculations were carried out using the 6-311+G(d, p) basis set, and the density-based implicit solvation model SMD was employed to describe the solvent effect of DMA:H₂O = 25:94. The interaction energies between H₂O and H₂O, and between DMA and H₂O, were calculated using the following formula

$$E_{\text{bind}} = E_{\text{complex}} - (E_{\text{partA}} + E_{\text{partB}}).$$

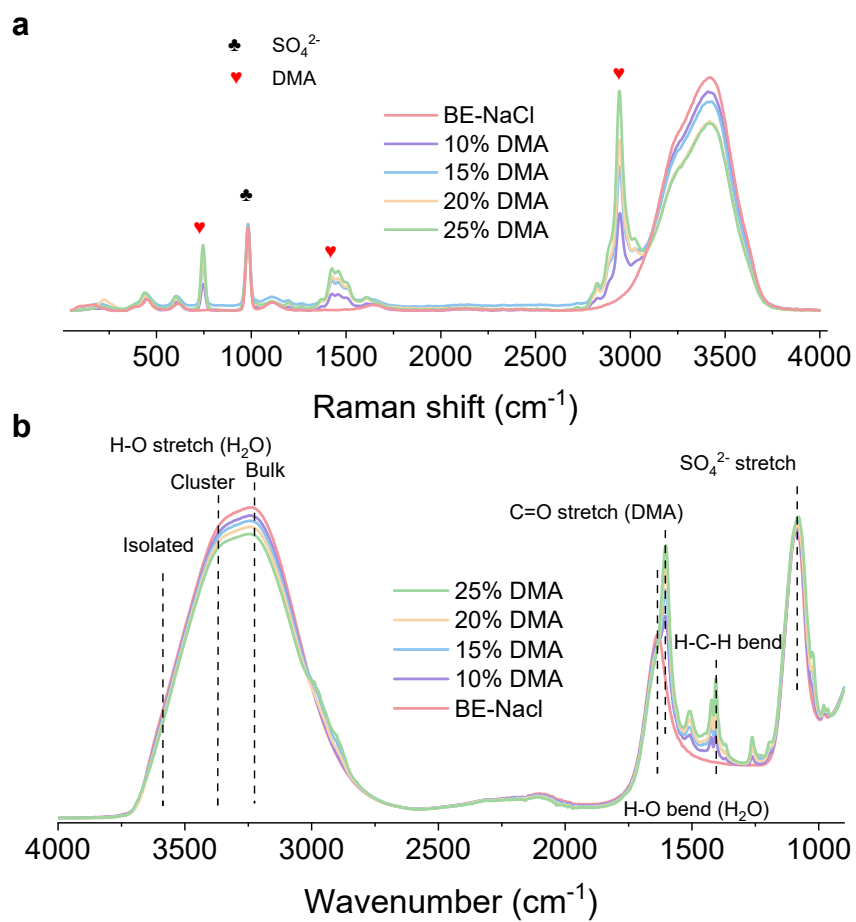


Fig. S1. The full (a) Raman and (b) FTIR spectra of BE-NaCl electrolytes with different concentration of DMA.

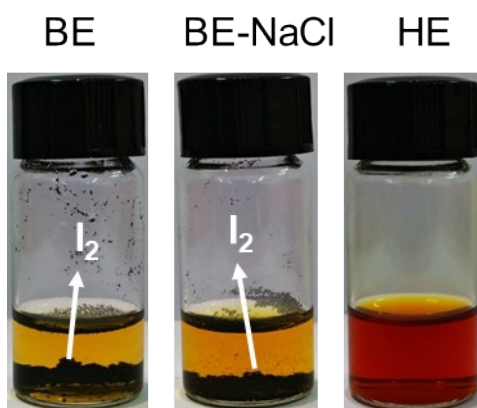


Fig. S2. Optical photograph of ICl added to different electrolytes.

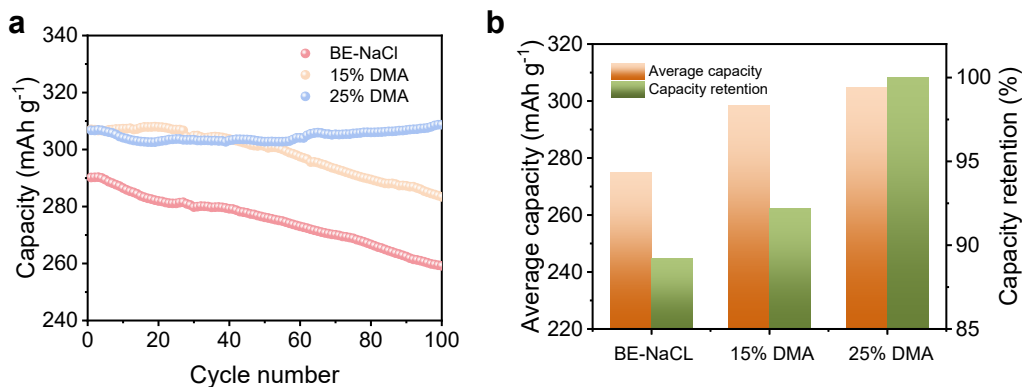


Fig. S3. (a) Cycling performance of Zn-I₂ batteries with BE-NaCl electrolytes containing different DMA concentrations at 1 A g⁻¹, (b) corresponding average discharge specific capacity and capacity retention of the batteries.

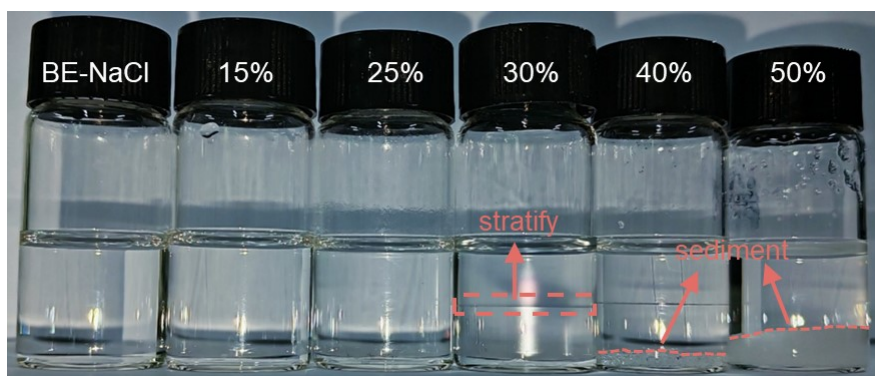


Fig. S4. Appearance of BE-NaCl electrolytes with varying DMA contents. Stratification occurs when DMA mass fraction exceeds 25%, and sedimentation appears with further increase in DMA content.

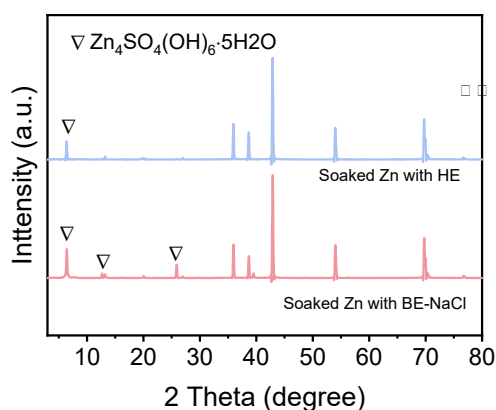


Fig. S5. XRD patterns of Zn foils after immersion in HE and BE-NaCl electrolytes.

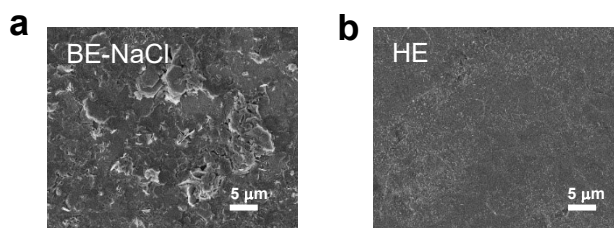


Fig. S6. SEM images of Zn foils after immersion in (a) BE-NaCl and (b) HE electrolytes.

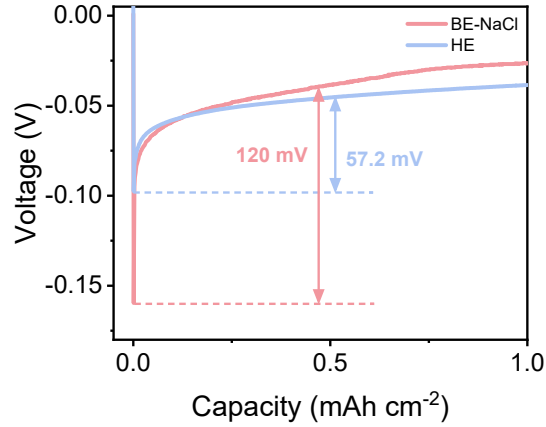


Fig. S7. Nucleation overpotential for the first Zn deposition.

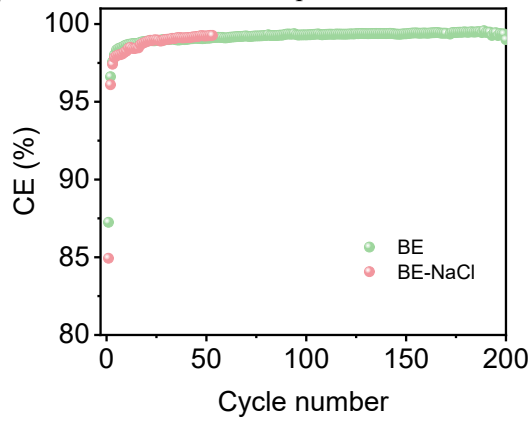


Fig. S8. CE values of Zn||Cu asymmetric cells at 1 mA cm⁻² and 1 mAh cm⁻².

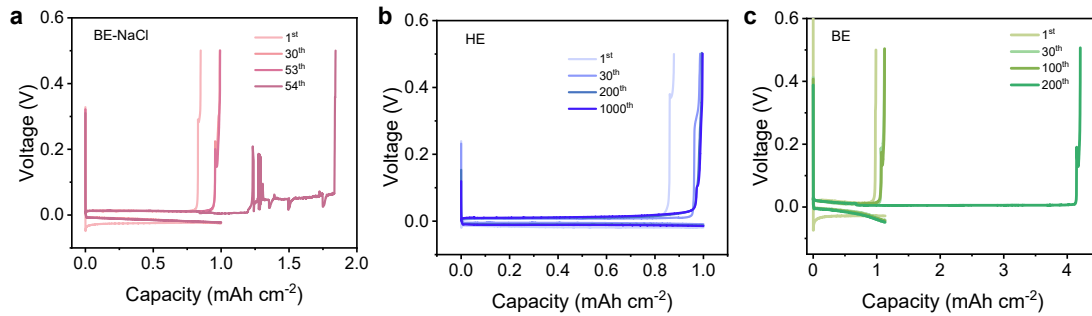


Fig. S9. Voltage profiles of a) BE-NaCl, b) HE and c) BE at a specific number of cycles.

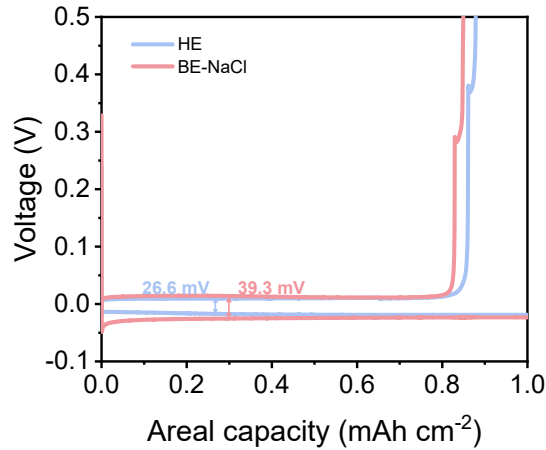


Fig. S10. Charge and discharge curves of Zn||Cu batteries.

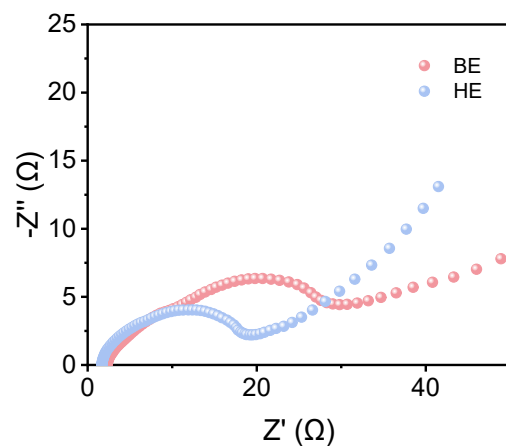


Fig. S11. Electrochemical impedance spectroscopy (EIS) Nyquist plots of Zn-I₂ batteries in BE and HE electrolytes.

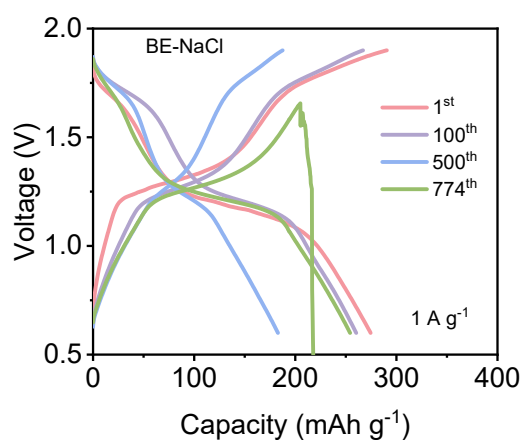


Fig. S12. Voltage profiles of Zn-I₂ battery in BE-NaCl electrolyte at a specific number of cycles.

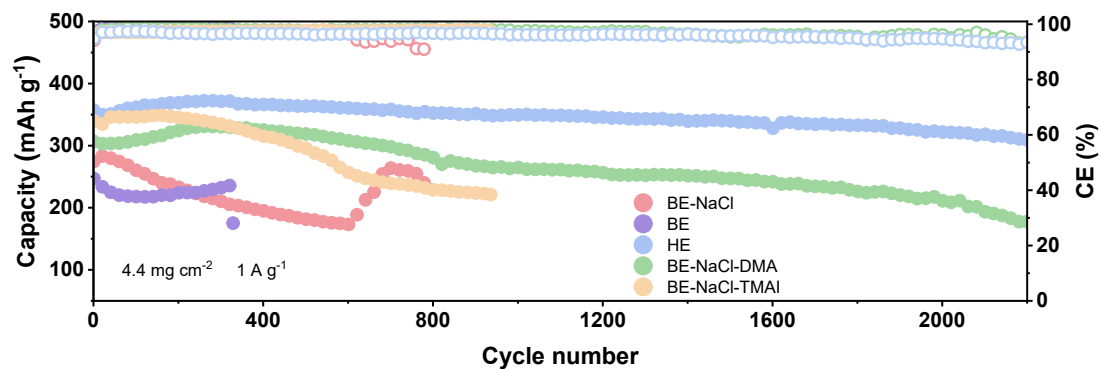


Fig. S13. Cycling performance of Zn||I₂ full cells in BE, BE-NaCl, BE-NaCl-DMA, BE-NaCl-TMAI and HE electrolytes at a current density of 1 A g⁻¹.

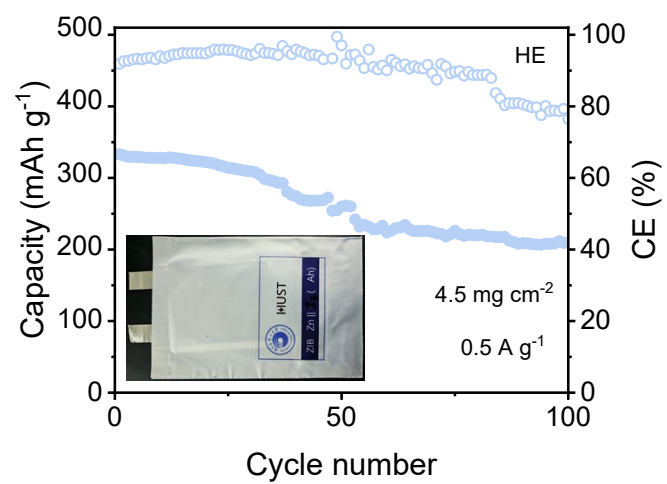


Fig. S14. Cycling performance of Zn-I₂ pouch cell in HE electrolyte at 0.5 A g⁻¹.